

# THE DIFFUSION PROCESS OF KITCHEN GAS EXHAUSTED TO THE OUTDOOR AIR SURROUNDING A MULTI-UNIT HOUSING FACILITY

Shinnichiro Nagano

FUJITA Corporation, Technology Research Institute

2025-1 Ono, Atsugi Kanagawa 243-0125, Japan

## ABSTRACT

This paper examines the process by which the kitchen exhaust from a dwelling unit diffuses throughout the other dwelling units in a seven-story housing facility. The diffusion process was examined by tracer gas measurements and compared to computer simulation. Results showed that kitchen gases exhausted from a central unit pollute all units on that entire floor and will vary in concentration depending on the wind direction.

## INTRODUCTION

We have often experienced that the smell of the kitchen exhaust from the other dwelling unit entered in our room on the multi-unit housing. This means that the outdoor air is not pure and contains the various materials generated by the cooking.

If the volatile organic compounds (VOCs) are generating from the building materials, the kitchen exhaust containing them pollutes the outdoor air and diffuses throughout the other dwelling units. The general multi-unit housings have the supply and the exhaust openings installed on the outside wall of the veranda side. Then, the ventilation of the dwelling units will be very likely to pollute the indoor air by VOCs in the outdoor air of the veranda side. Therefore, the ventilation systems of the multi-unit housing have better design in consideration of the diffusion process of the exhaust air from each dwelling unit. The investigation of prediction on the building surface concentrations is Ohba(1998). In this paper, the tracer gas measurements and computer simulations have examined to clarify the diffusion process of kitchen exhaust on the veranda side of a multi-unit housing.

## MEASUREMENT

The case study building with seven floors is located in Tokyo and has the 25 dwelling units on floors 3 through 7. The veranda between the dwelling units has been partitioned by a simple frame wall and faces east. Figure 1 shows the outward appearance of the case study building. The tracer gas concentrations were measured for the ten veranda positions as shown in Figure 2 and for the indoor air of the dwelling unit 403 and the kitchen exhaust gas. The rooftop wind speed and direction was measured on

the height of 5 m above the roof floor.

The measuring systems were composed of the B&K TYPE 1302 and 1312. The used tracer gas was SF<sub>6</sub> raw gas of 99.99% and was injected in the kitchen exhaust of the dwelling unit 403 at 150 cc/min. The exhaust range fan was running continuously in the measurement period. The concentrations versus time were measured at the veranda side during about 7 hours including from the beginning of the gas mixing to the end. The kitchen exhaust SF<sub>6</sub> concentration at steady-state was 24 ppm and the indoor SF<sub>6</sub> concentration was 6 ppm. Therefore, the exhaust gas volume from the kitchen range was 511 m<sup>3</sup>/h.

## MEASUREMENT RESULTS

Figure 3 shows the meteorological conditions for the measurement period of 8/12-8/13 in 1998. The wind direction was almost SSW, and the averaged wind speed was 2m/s. The outdoor air temperature was falling down in the measuring period gradually.

Figure 4(a) shows the SF<sub>6</sub> concentrations versus time at the measurement points. The concentrations of each dwelling unit reaches almost steady-state after about 1 hour from the beginning of SF<sub>6</sub> injection. The veranda concentration of the dwelling unit 403 (403v) is fluctuating a little higher than the other concentrations of the veranda measurement points. The concentrations of 401 and 402 show a little higher than that of 403. The concentrations of each



Figure 1 The 7-story case study building seen from the veranda side.

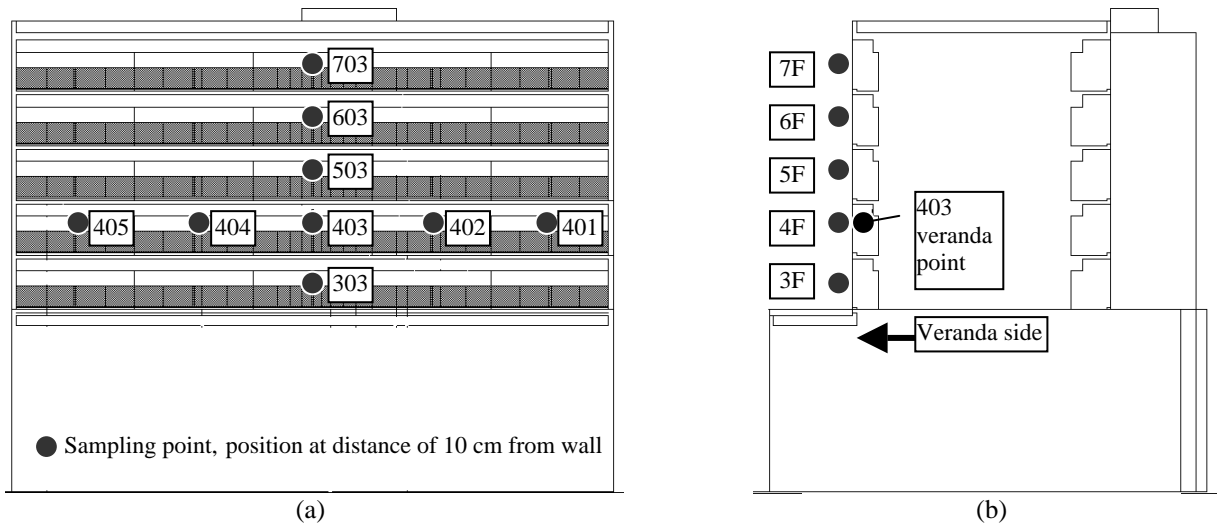


Figure 2 The case study building showing living units on floors 3 through 7. (a) Façade showing the measurement positions, (b) Transverse cross-sectional view.

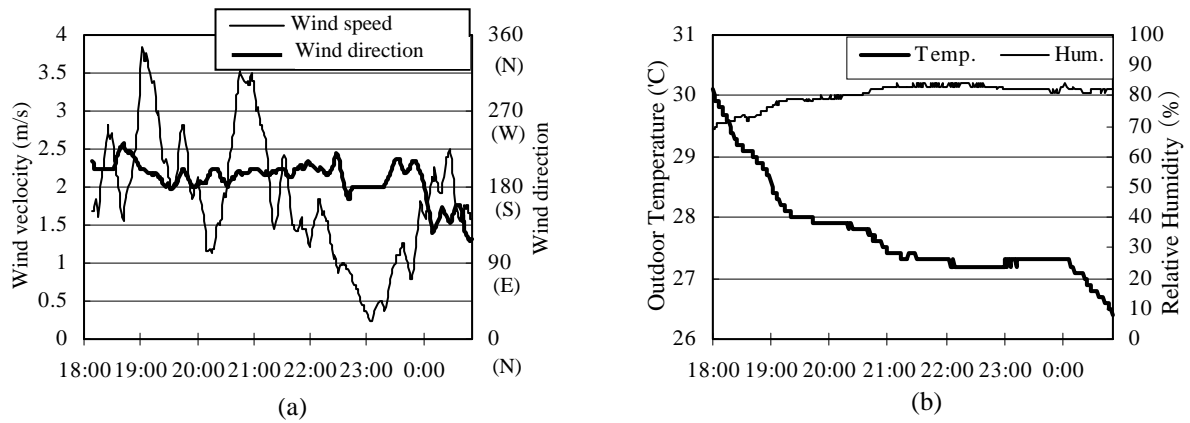


Figure 3 Meteorological conditions for the measurement period of 8/12-8/13 in 1998. (a) Wind speed and direction, (b) Air temperatures and relative humidity.

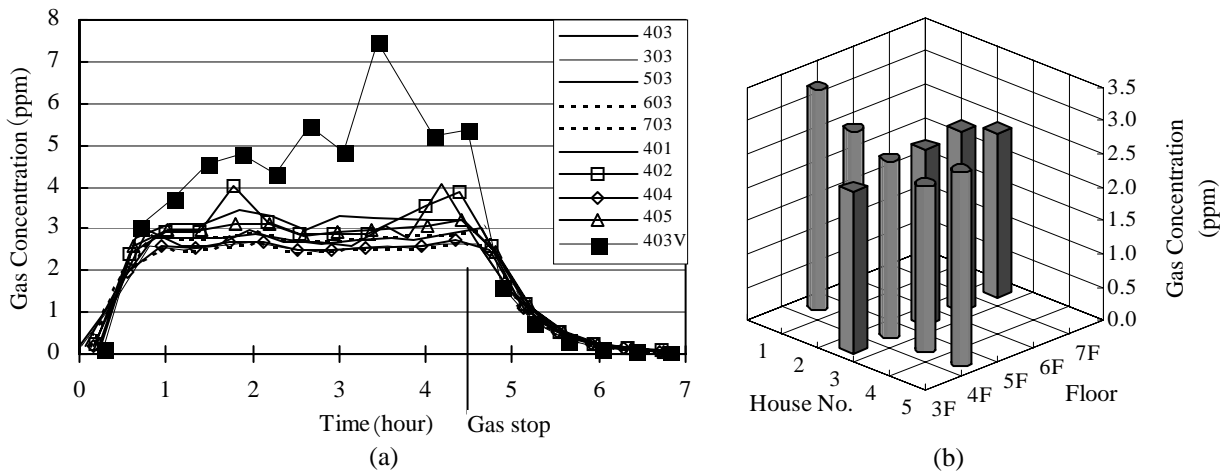


Figure 4 Measured tracer gas concentrations at the 10 measuring points. (a) Concentration vs. time, (b) The 180-minute steady-state concentration.

measurement point reaches nearly zero after about two and a half-hours from the end of the SF6 injection. The decreasing patterns of each concentration are almost the same.

Figure 4(b) shows the 180-minute steady-state

concentration from the beginning of SF6 injection. The concentrations of 401 and 405 are higher than that of 403 in the horizontal direction, while the concentrations of 303-703 in the vertical direction are the same value.

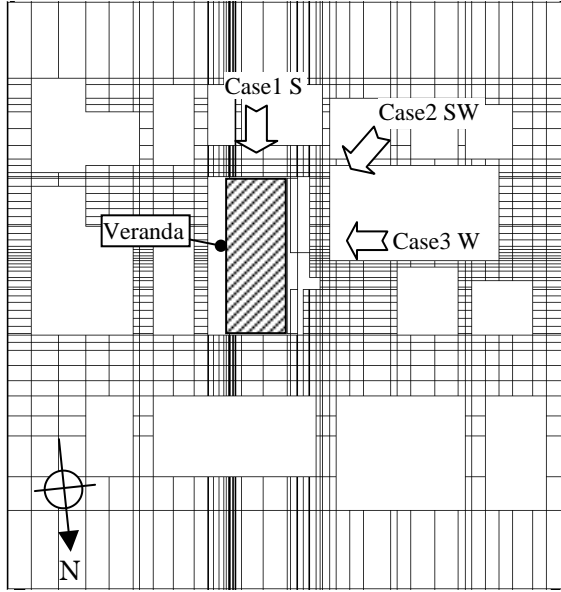


Figure 5 Mesh definition for analysis of wind directions among the surrounding buildings.

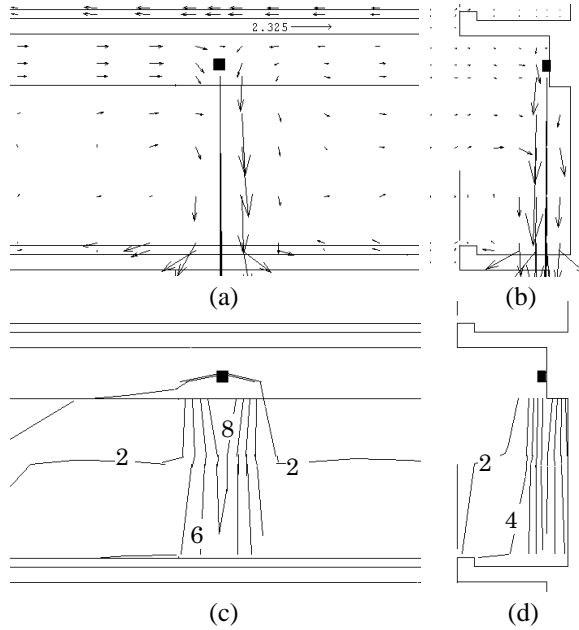


Figure 6 Perpendicular section airflow and concentration distribution of kitchen exhaust of dwelling unit 403, (a) Parallel airflow distribution in window, (b) airflow distribution in veranda section, (c) Parallel concentration distribution in window, (d) Concentration distribution in veranda section. (unit : ppm)

Table 1 Modeled cases.

Case 1	South wind
Case 2	Southwest wind
Case 3	West wind

$$\frac{\partial \langle u_i \rangle}{\partial x_i} = 0 \quad \dots(1)$$

$$\frac{\partial \langle u_i \rangle}{\partial t} + \frac{\partial \langle u_i \rangle \langle u_j \rangle}{\partial x_j} = -\frac{\partial}{\partial x_i} \left( P + \frac{2}{3} k \right) + \frac{\partial}{\partial x_j} \left\{ v_i \left( \frac{\partial \langle u_i \rangle}{\partial x_j} + \frac{\partial \langle u_j \rangle}{\partial x_i} \right) \right\} \dots(2)$$

$$\frac{\partial k}{\partial t} + \frac{\partial k \langle u_j \rangle}{\partial x_j} = \frac{\partial}{\partial x_j} \left( \frac{v_i}{\sigma_i} \frac{\partial k}{\partial x_j} \right) + P_k - \varepsilon \quad \dots(3)$$

$$\frac{\partial \varepsilon}{\partial t} + \frac{\partial \varepsilon \langle u_j \rangle}{\partial x_j} = \frac{\partial}{\partial x_j} \left( \frac{v_i}{\sigma_2} \frac{\partial \varepsilon}{\partial x_j} \right) + C_1 \frac{\varepsilon}{k} P_k - C_2 \frac{\varepsilon^2}{k} \quad \dots(4)$$

$$\frac{\partial C}{\partial t} + \frac{\partial C \langle u_j \rangle}{\partial x_j} = \frac{\partial}{\partial x_j} \left( \frac{v_i}{S_c} \frac{\partial C}{\partial x_j} \right) \dots(5) \quad P_k = C_\mu \frac{k^2}{\varepsilon} S \Omega \quad \dots(6)$$

$$S = \sqrt{\frac{1}{2} \left( \frac{\partial \langle u_i \rangle}{\partial x_j} + \frac{\partial \langle u_j \rangle}{\partial x_i} \right)^2} \quad \dots(7) \quad \Omega = \sqrt{\frac{1}{2} \left( \frac{\partial \langle u_i \rangle}{\partial x_j} - \frac{\partial \langle u_j \rangle}{\partial x_i} \right)^2} \quad \dots(8)$$

$$S = \min(20, S) \quad \dots(9) \quad C_\mu = \min \left( 0.09, \frac{0.3}{1 + 0.35 S^{1.5}} \right) \quad \dots(10)$$

$$\sigma_1 = 1.0, \sigma_2 = 1.3, C_1 = 1.44, C_2 = 1.92, S_c = 0.9$$

Figure 7 Modified production k-ε model equations

**Inflow boundary**<sup>2)</sup>:

$\langle u_i(x_3) \rangle, k(x_3)$ :

(1)  $x_3 \geq 0.08$      $\langle u_1(x_3) \rangle = x_3^\alpha$  ( $\alpha = 0.20$ )  
 $k(x_3) = -0.00703 x_3 + 0.0091$

(2)  $x_3 < 0.08$      $\frac{\langle u_1(x_3) \rangle}{u_*} = \frac{1}{\kappa} \ln \frac{x_3}{z_0}$   
 $k(x_3) = -0.607 x_3^2 + 0.0960 x_3 + 0.00466$   
 where  $\kappa = 0.4, u_* = 0.0278, z_0 = 5.0 \times 10^{-5}$

$\langle u_2 \rangle = 0, \langle u_3 \rangle = 0, \varepsilon(x_3) = C_\mu k(x_3)^{3/2} / l(x_3)$

$l(x_3) = (C_\mu k(x_3))^{1/2} \left( \frac{\partial \langle u_1(x_3) \rangle}{\partial x_3} \right)^{-1}$

**Outflow boundary:** free-slip

**Wall boundary:**

$$\frac{\langle u_i \rangle_p}{u_*} = \frac{1}{\kappa} \ln \frac{u_*}{v} \frac{h_p}{2} + 5.5 \quad k_p = \frac{u_*^2}{\sqrt{C_\mu}} \quad \varepsilon_p = \frac{u_*^3}{\kappa \frac{1}{2} h_p}$$

**Kitchen exhaust condition:**

- supply velocity 28.4 (m/s) downward direction
- supply air volume 511 (m<sup>3</sup>/h)
- supply gas concentration 24 (ppm)
- supply opening configuration 0.1(m)\*0.05(m)

Figure 8 Equations for the boundary conditions

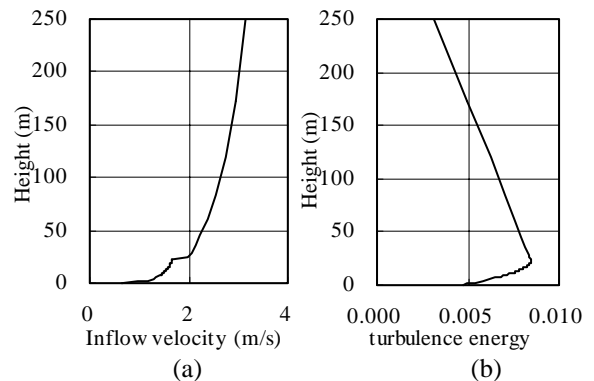


Figure 9 Profiles of air inflow velocity and turbulent energy

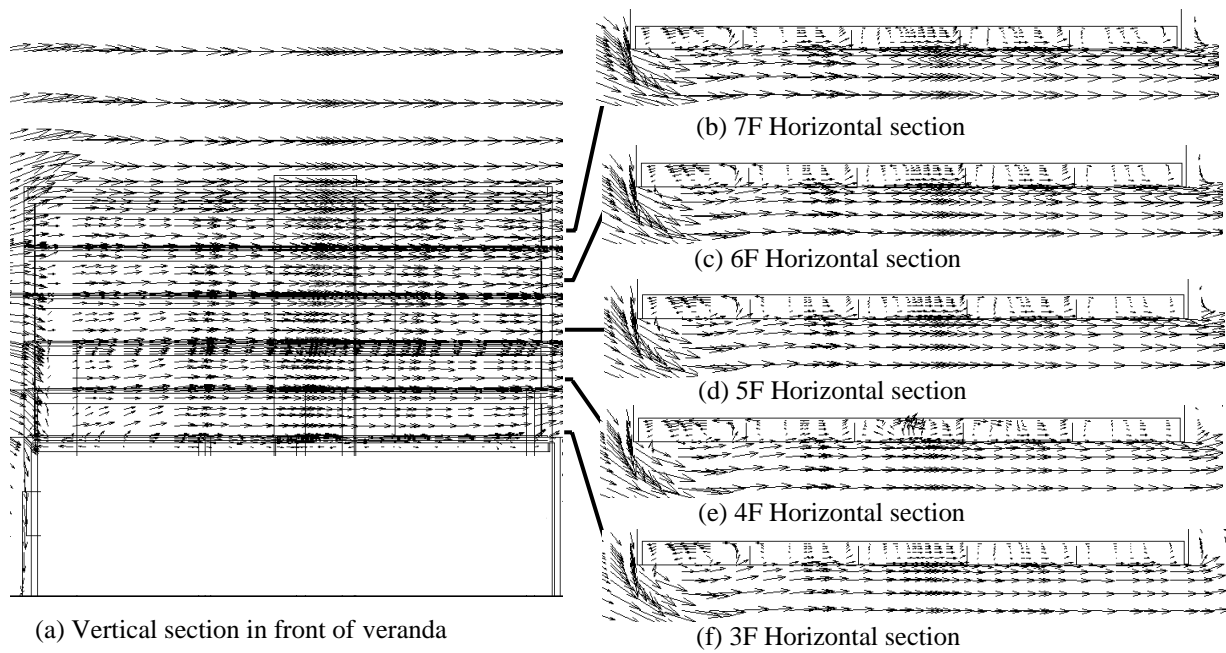


Figure 10 Simulated airflow patterns for a south wind. Air moves to the veranda in parallel pattern toward the right as the wind enters from the left.

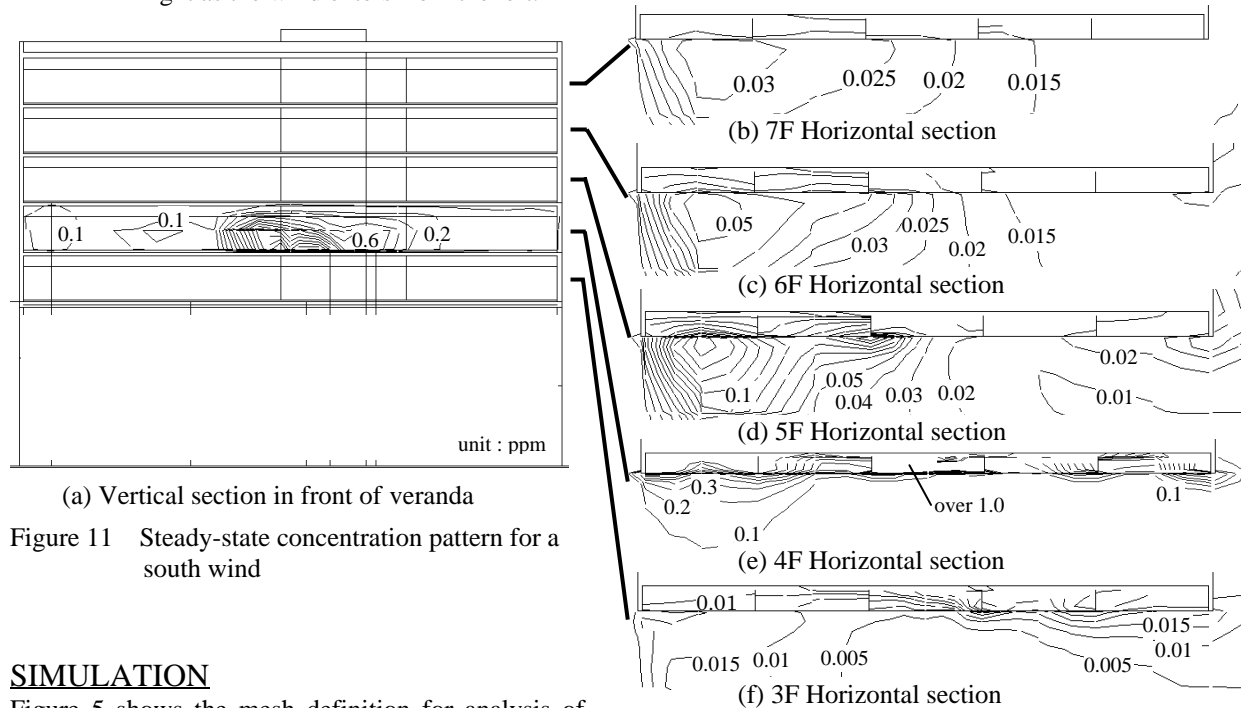


Figure 11 Steady-state concentration pattern for a south wind

## SIMULATION

Figure 5 shows the mesh definition for analysis of wind directions among the surrounding buildings. The analysis region size is 500m(L) × 500m(W) × 300m(H) around the case study building, and the mesh size is 240,400 (60(x) × 64(y) × 60(z)). The diffusion processes of the gas concentration are investigated about three wind directions of South, Southwest and West as shown in Table 1.

Figure 6 shows the airflow and concentration patterns around the kitchen exhaust opening of the dwelling unit 403. The simulation results in this paper are obtained by used 'STREAM' of commercialized software. The airflow patterns are simulated by the isothermal modified production k-ε model (hereafter,

MP k-ε model) as shown in Figure 7. The boundary conditions are shown in Figure 8. The MP k-ε model has the effect to improve the production term of turbulent energy in the place where the wind collides with the building. The gas behavior is treated as passive scalar contaminant.

The convection term of the velocity is solved by the QUICK scheme and that of the concentration is solved by the upwind scheme. The steady-state concentration pattern is solved after the airflow field data in steady-state are obtained. Figure 9 shows the profiles of air inflow velocity and turbulent energy.

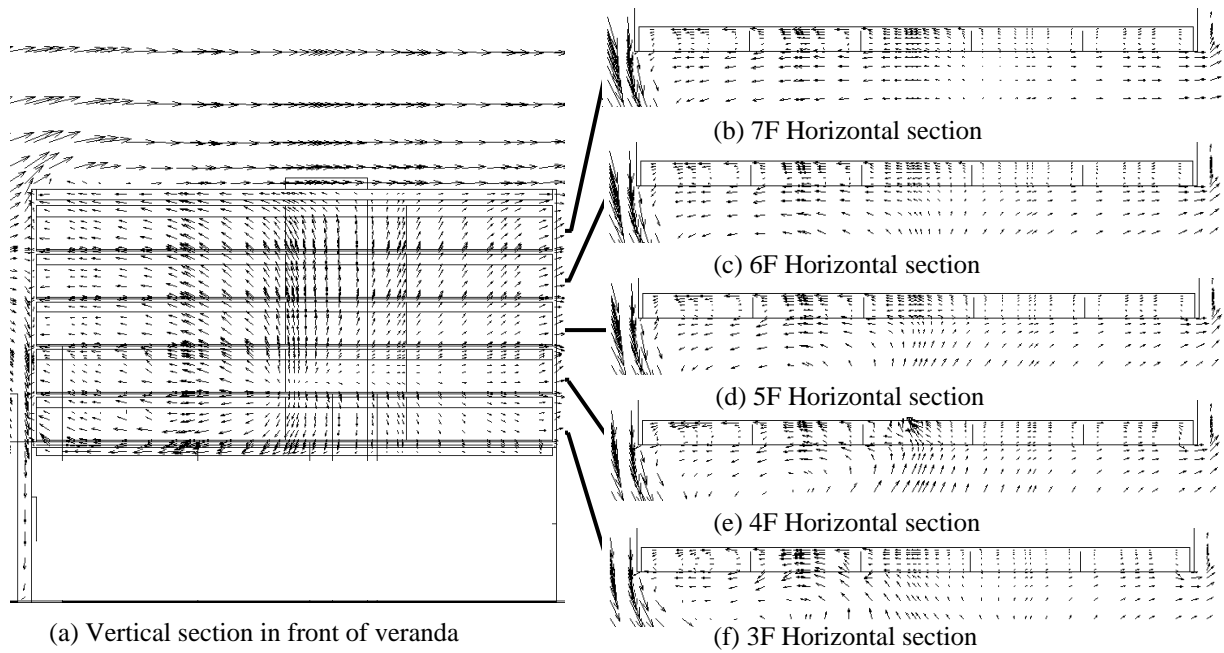


Figure 12 Simulated airflow pattern for a southwest wind showing a vortex formed by the handrail at the left side of the building.

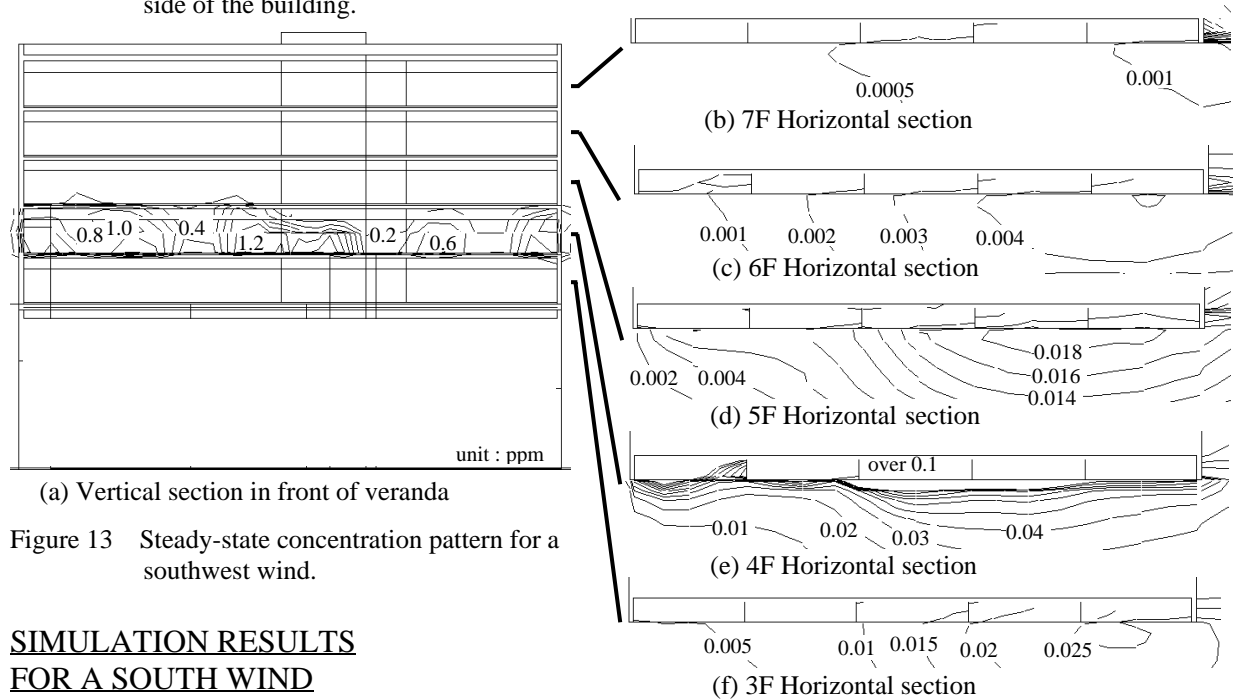


Figure 13 Steady-state concentration pattern for a southwest wind.

**SIMULATION RESULTS FOR A SOUTH WIND**

Figure 10 shows the airflow patterns for a south wind in the vertical section and the horizontal section of each floor in front of veranda and Figure 11 shows the steady-state concentration patterns for that. The air moves to the veranda in parallel pattern toward the right as the wind enters from the left. The wind impinged on the left outdoor wall of the building and the vortex is formed in front of the veranda as the result. As the simple frame wall in the veranda of each dwelling unit blocks the airflow, the recirculation flows are formed in the veranda of each dwelling unit.

The high-level concentration pattern appears around the dwelling unit 403, particularly in horizontal

direction of the fourth floor as shown in Figure 11(a) and Figure 11(e). When the kitchen exhaust is left untransported in the vortex of the veranda side, the outdoor concentrations in the vortex would be increasing to some extent. The vortex plays an important part in spreading the kitchen exhaust horizontally.

Therefore, the kitchen exhaust from a dwelling unit can be easy to pollute the veranda air of the other dwelling units on the same floor. The high-level concentration region appearing in the windward system has the influence on the design of ventilation system because of the air polluting toward the windward

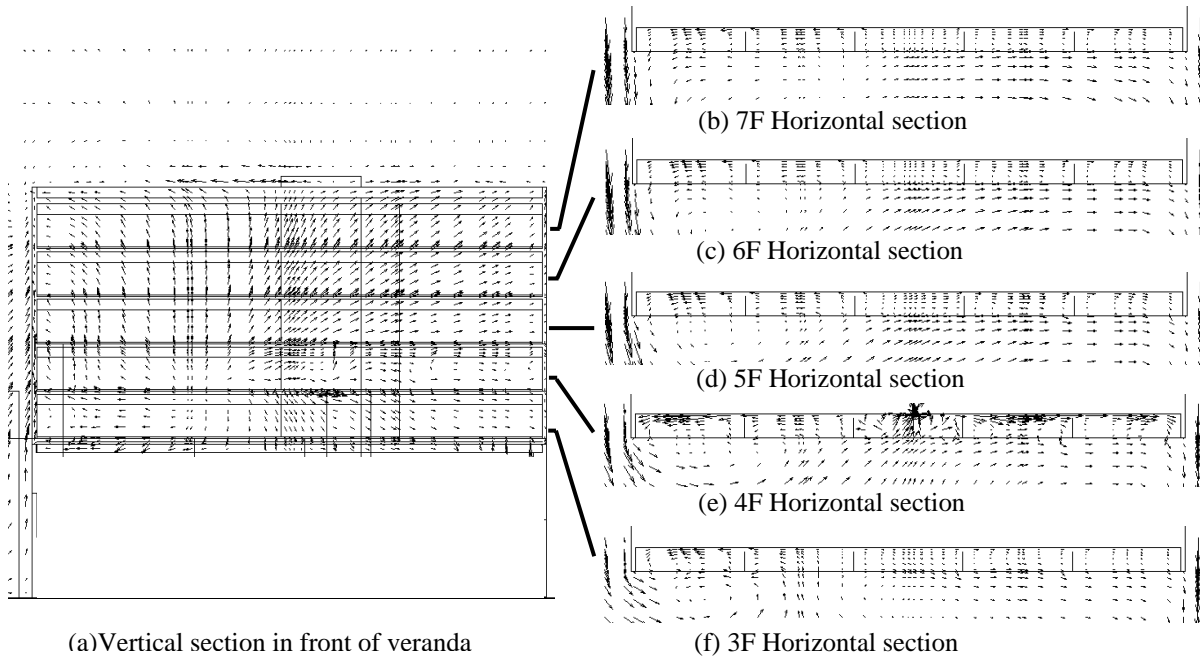


Figure 14 Simulated airflow pattern for a west wind. Air moves from the back toward the front of the building causing a wake on the veranda side.

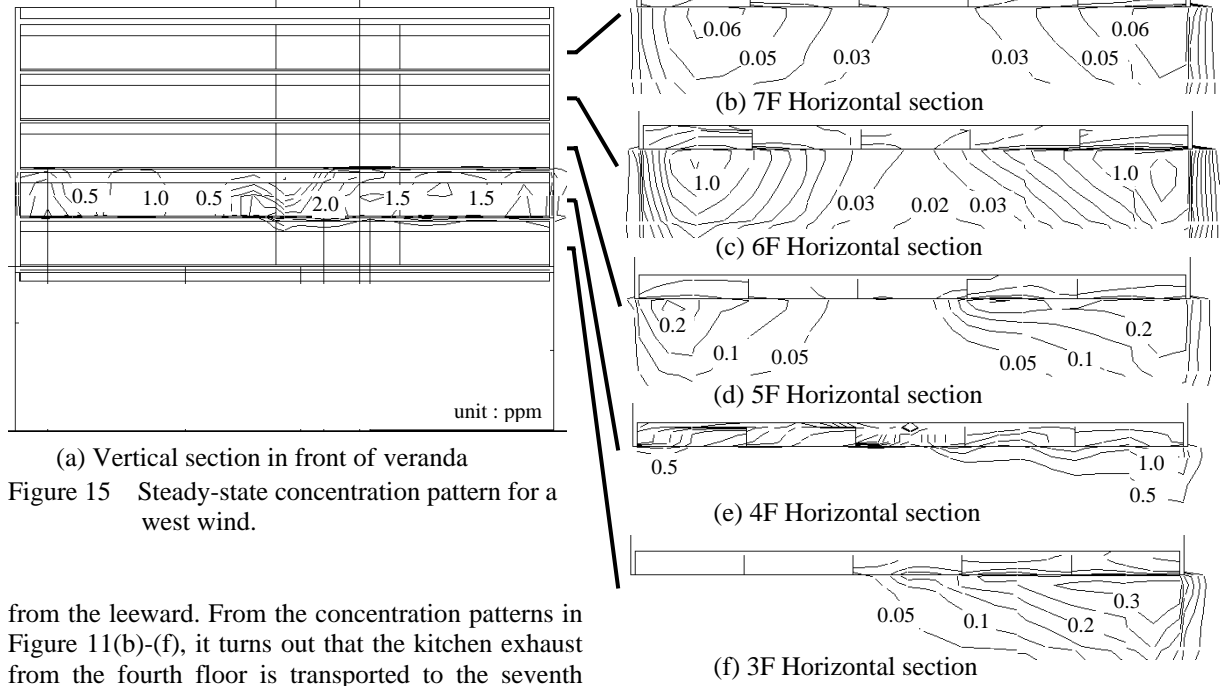


Figure 15 Steady-state concentration pattern for a west wind.

from the leeward. From the concentration patterns in Figure 11(b)-(f), it turns out that the kitchen exhaust from the fourth floor is transported to the seventh floor by an upward wind.

**FOR A SOUTHWEST WIND**

The airflow pattern for a southwest wind is shown in Figure 12 and the concentration pattern for that is shown in Figure 13. The airflow pattern shows a vortex formed by the handrail at the left side of the building. The vortex is larger than that for a south wind and holds one side of the building. The airflow direction of veranda side forks at the center of the building as shown in Figure 12. The concentration of veranda on fourth floor with dwelling unit 403 is very higher than that on other floor as shown in

Figure 13(a). The concentration patterns have clustered on the leeward of building as shown in Figure 13(b)-(f).

**FOR A WEST WIND**

The airflow pattern is shown in Figure 14, and the concentration pattern is shown in Figure 15. As air moves from the back toward the front of the building causing a wake on the veranda side, two vortices are formed on both sides of the building. The airflow becomes the downward flow at third floor and the upward flow above the fifth floor in Figure 14(a). In

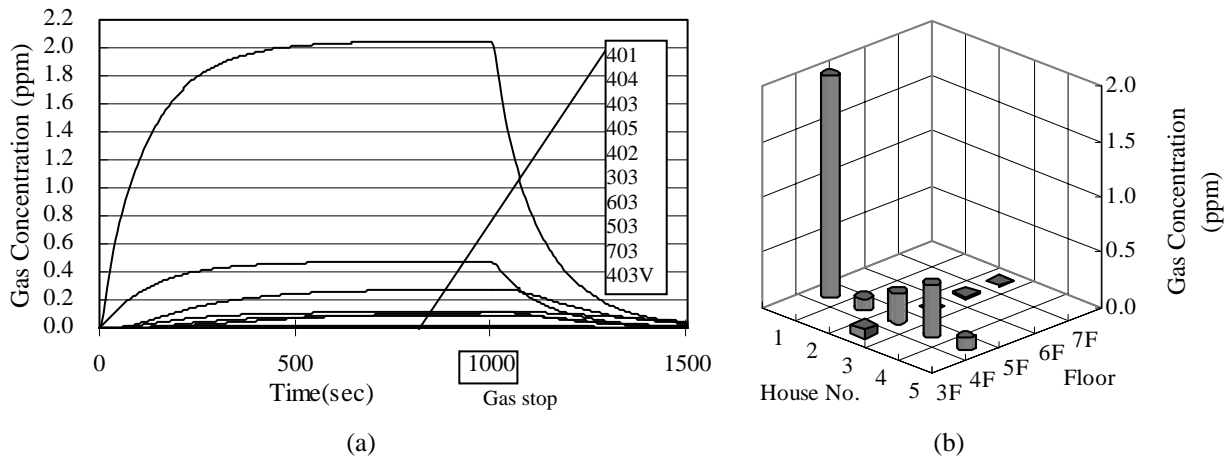


Figure 16 Gas concentrations for a south wind, simulated by MP k-ε model at the 10 points. (a) Concentration vs. time, (b) The steady-state concentration.

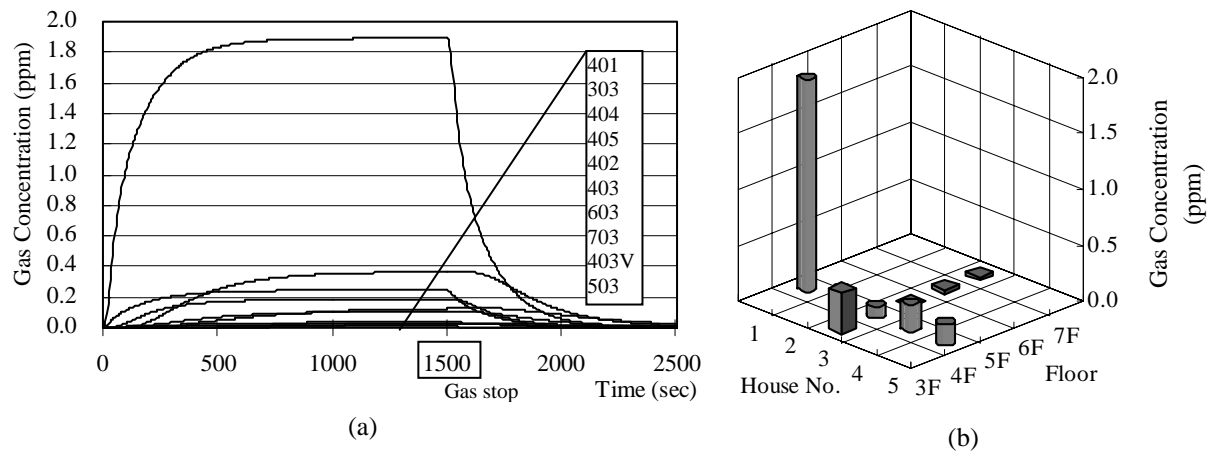


Figure 17 Gas concentrations for a southwest wind, simulated by MP k-ε model at the 10 points. (a) Concentration vs. time, (b) The steady-state concentration.

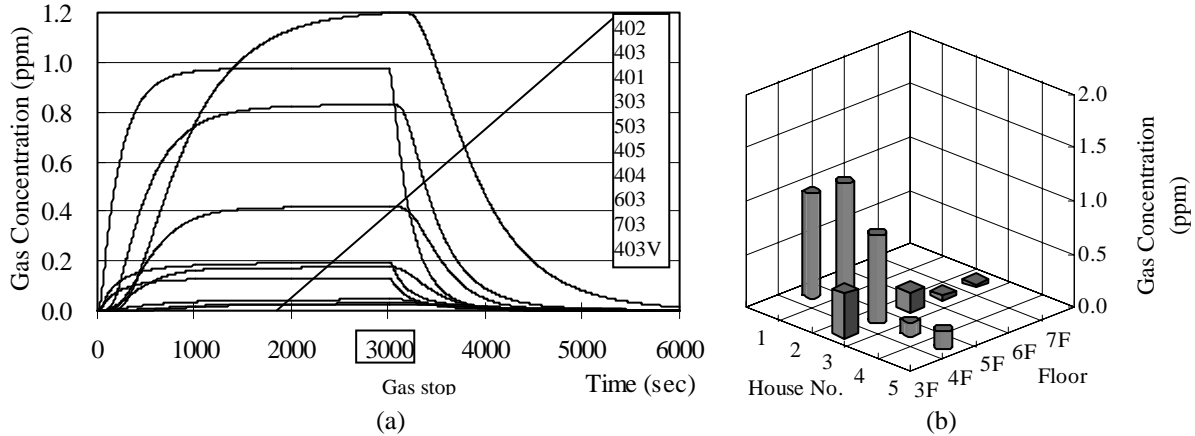


Figure 18 Gas concentrations for a west wind, simulated by MP k-ε model at the 10 points. (a) Concentration vs. time, (b) The steady-state concentration.

addition, the airflow shows the unsymmetrical pattern in vertical section in front of veranda in Figure 14(b)-(f). The concentration patterns above the fifth floor show the high-level polluted regions where the vortices are formed on both sides of the

building. The gas injected in veranda of dwelling unit 403 results in diffusing in the horizontal direction on fourth floor and in the both ends of building by

vortexes on both sides.

### CHANGE AT CONCENTRATION

Figure 16-18 show the concentration versus time for three wind directions simulated by MP k-ε model.

### FOR A SOUTH WIND

The gas concentrations for a south wind shown in

Figure 16. The gas injection is continued to 1,000 seconds. The concentration of dwelling unit 401 on the leeward is highest than that of the other dwelling units, while dwelling units except for 401 show the same low-level concentration. The simulated concentrations become lower than the measurement results (Figure 4) for a same wind direction. The simulated concentrations between each sampling point have a difference, while the measurement concentrations are equal in level. In addition, the maximum value indicates on 403 by measurement and on 401 by simulation.

### FOR A SOUTHWEST WIND

The gas concentrations for a southwest wind are shown in Figure 17. The gas injection is continued to 1,500 seconds. The concentration of 401 indicates the maximum value and that of 303 is the next. The vortex formed on the zone in front of 401 veranda confines the gas to the space and keeps in the high level concentration in 401 veranda. Though the concentration of 303 is lower than that of 404 and 405 just after gas injection, it becomes higher than them in steady-state. In addition, the concentration of 303 keeps in a high level after gas stops. It means that air in there is likely to hang comparison with the other point.

### FOR A WEST WIND

Figure 18 shows the gas concentrations for a west wind. The gas injection is continued to 3,000 seconds. The concentrations of each dwelling unit for a west wind are higher than that for a south and southwest wind. The concentration of dwelling unit 401 reaches to the maximum after 1,000 seconds from the beginning of gas injection. On the contrary, the concentration of dwelling unit 402 shows the highest value after about 1,400 seconds and is increasing to gas stop. After gas stop, the concentration of 401 becomes decreasing rapidly and reaches to nearly zero faster than that of 403 and 303.

### CONSIDERATION

The diffusions of the kitchen exhaust in the wake of building showed the very interesting behavior for three wind directions. The simulated steady-state concentrations for a south wind regretfully were not equivalent for the measurements. The reason is that wind direction versus time is always changing as shown in Figure 3(a), but it is regarded a constant wind direction in simulation. Another reason is thought that it is overestimated the diffusion of the concentration by the rough mesh division.

### CONCLUSIONS

The diffusion process of the kitchen gas exhausted from a dwelling unit almost centered on a multi-unit housing was examined by tracer gas measurements and compared to computer simulation. The

conclusions are as follows.

1) The measurement results for a south wind showed almost the same concentration level in front of the veranda of each dwelling unit. In that case, the simulated concentrations of veranda on each dwelling unit were lower than the measurement concentrations.

2) The kitchen exhaust from a dwelling unit is likely to pollute the outdoor air of the neighboring unit. The concentration patterns are showing a tendency to spread in horizontal direction along veranda.

3) The vortex formed on the zone in front of veranda plays a part in keeping the high-level concentration pattern.

4) The concentration versus time and the steady-state concentration in front of veranda depend on a wind direction. In particular, the gas concentrations in wake for a west wind are higher than that of the other wind (S,SW). The difference between measurement and simulation will be improved by reconsidering the inflow condition and turbulence model in future.

### REFERENCES

- 1) OHBA, M "Wind tunnel experiments on flow fields around twin high-rise building models Part3", proceedings of 15<sup>th</sup> national symposium on wind engineering, 1998
- 2) SAKAGUCHI, J. and S. AKABAYASHI et al., "Research on the prediction technique of a change in a wind environment by the middle layer building", summaries of annual meeting of AIJ, D-2, 1998.